

# EFFECTS OF GRAVITY ON TRIPLE FLAME PROPAGATION AND STABILITY

J.-Y. Chen<sup>1</sup>, Tarek Echekki<sup>2</sup>, and Uday Hegde<sup>3</sup>, <sup>1</sup>6163 Etcheverry Hall, University of California at Berkeley, Berkeley, CA 94720-1740, [jychen@newton.me.berkeley.edu](mailto:jychen@newton.me.berkeley.edu), <sup>2</sup>Combustion Research Facility, MS 9051, Sandia National Laboratories, Livermore, CA 94551-0969, [techekk@ca.sandia.gov](mailto:techekk@ca.sandia.gov), <sup>3</sup>National Center for Microgravity Research, NASA Glenn Research Center, Cleveland, OH 44135, [uday.hegde@grc.nasa.gov](mailto:uday.hegde@grc.nasa.gov)

## INTRODUCTION

Numerical simulations of 2-D triple flames under gravity force have been implemented to identify the effects of gravity on triple flame structure and propagation properties and to understand the mechanisms of instabilities resulting from both heat release and buoyancy effects. A wide range of gravity conditions, heat release and mixing widths for a scalar mixing layer are computed for downward-propagating (in the same direction with the gravity vector) and upward-propagating (in the opposite direction of the gravity vector) triple flames.

## TRIPLE FLAME PROPAGATION

Simulations of planar triple flames in a scalar-mixing layer are implemented [1,2]. A single fuel and oxidizer are considered with unity Lewis numbers and a simple irreversible reaction with unitary stoichiometric coefficients. The compressible Navier-Stokes equations along with the conservation equations for species and energy are solved in a two-dimensional domain. Spatial derivatives are approximated with a sixth-order compact finite-difference algorithm. Temporal integration is performed using a low-storage third-order Runge-Kutta scheme. Boundary conditions are specified using the Navier-Stokes Characteristic Boundary Conditions (NSCBC) [3]. The flame is stabilized using a procedure similar to the one implemented by Ruetsch *et al* [4]. A correction is applied to the streamwise component of the velocity field such that temperature contours in the leading edge of the reaction zone are fixed at the same location. The inlet velocity is adjusted accordingly; while, the mass fraction at the inlet is specified with an error function profile. The solutions are allowed to evolve until steady-state of the flame structure is reached.

Figure 1 presents the computed contours of fuel consumption rate in a two-dimensional domain. The mixture enters the domain from the left side of the boundary. As seen in the reaction rate contour, the triple flame structure is delineated by its three branches. The two “wings” correspond to the lean and rich premixed flames. The “tail” trailing the premixed branches corresponds to the diffusion flame where excess fuel and oxidizer from the premixed branches are burned. As the triple flame propagates upstream, the flow ahead of the triple flame tip is decelerated as streamlines diverge. Near the reaction zone, heat release causes the flow to accelerate. Further downstream of the triple flame tip, the flow gradually decelerates as the flow behind the flame tip continues to expand laterally.

The propagation speed of the triple flame is computed by tracking an interface corresponding to a fixed fuel mass fraction along the centerline. The corresponding displacement speed,  $S_D$ , of this interface along the centerline in the streamwise is related to the triple flame propagation speed,  $S_p$ , using the following relation:

$$S_p = (S_D - u) + u_0, \quad (1)$$

where  $u$  is the streamwise velocity component at the interface and  $u_0$  is the inlet velocity, both evaluated at the centerline. A series of simulations have been conducted to explore the relation between the triple flame propagation speed and the Froude number,  $Fr_{L_f} = S_L^2/gL_f$ , based on the flame thickness,  $L_f$ .  $S_L$  is the laminar flame speed and  $g$  is the gravity acceleration. The value of  $g$ , and accordingly the value of the Froude number, is positive in downward-propagating flames and negative in upward-propagating flames. The run conditions are summarized in Table 1.

Case	$\alpha$	$W/L_f$	$S_L/S_L(A)$	$\rho_0/\rho_\infty$	$1/Fr_{L_f}$
A	0.85	2	1	6.67	(-1.0→0.5)
B	0.85	4	1	6.67	(-0.5→0.5)
C	0.85	8	1	6.67	(-1.0→0.625)
D	0.70	4	1	3.34	(-1.0→0.5)
E	0.85	3.2	0.8	6.67	(-0.938→0.547)
F	0.85	4.8	1.2	6.67	(-0.417→0.365)

**Table 1.** Simulation conditions. Under all conditions, the Zel'dovich number is 8.  $\alpha$  is the heat release parameter that corresponds to the ratio between the flame temperature to the difference between the flame temperature (denoted with subscripts  $\infty$ ) and unburnt gas temperature (denoted with subscripts 0) at stoichiometric conditions.  $W$  is the scalar mixing layer width. All flame speeds shown are normalized with the value in case A. ( $a \rightarrow b$ ) corresponds to a range of values between  $a$  and  $b$ .

Comparisons of the contributions of the local gas velocity and the displacement speed to  $S_p$  shows that the enhancement of  $S_p$  due to buoyancy effects may be attributed primarily to buoyancy-induced flow acceleration. A simple analytical model for the triple flame speed, which accounts for both buoyancy and heat release, is developed [1]. The model formulation yields the following relation between the triple flame speed and gravity in the limit of small gravity force:

$$\frac{S_p}{S_{p,g=0}} \approx \left( 1 - C_0 \frac{\rho_\infty}{\rho_0} \frac{1}{Fr_{L_f}} \right)^{1/2} \equiv \sqrt{1 - X}, \quad (2)$$

where  $C_0$  is a constant to be determined and  $X \equiv C_0 (\rho_\infty/\rho_0)(1/Fr_{L_f})$ . Although this correlation is limited to small values of the parameter,  $X$ , its predictions of the general trends of the triple flame propagation speed may extend beyond its underlying assumptions. First, the relation predicts the behavior of the flame at the limiting conditions of zero gravity. The expression also shows that the triple flame speed is enhanced by gravity in upward-propagating flames and reduced in downward propagating flames. As in the original analysis of Ruetsch *et al* [4], lateral flow expansion is the primary mechanism for triple flame speed enhancement, and through which heat release (expressed here in terms of the density ration,  $\rho_\infty/\rho_0$ ) appears in the expression for the triple flame speed. Buoyancy, then, acts to modulate this expansion by fluid acceleration or deceleration through the flame. Finally, the above equation suggests the existence of a critical value for  $Fr_{L_f}$  in downward propagating flames for which the triple flame propagation speed approaches zero:

$$Fr_{L_f, critical} \approx C_0 \frac{\rho_\infty}{\rho_0}, \quad \text{or} \quad g_{critical} \approx \frac{\rho_0}{\rho_\infty} \frac{S_L^2}{L_f}. \quad (3)$$

Results of the analysis are compared to the simulations summarized in Table 1. Figure 2 presents a comparison of computed triple flame propagation speeds and the simplified model with  $C_0 = 10$ . The agreement is good except for large values of  $X$  where the assumption of small gravity force is not valid. Also indicated in the figure are the estimated ranges for stoichiometric methane-air combustion and those with a fuel mixture of 77%  $N_2$  and 23%  $H_2$  by volume. The latter has the same laminar flame speed as methane-air premixed flame but with a thickness about four times larger. These estimates are seen to fall into the regions where Equation 2 is accurate. Consequently, Equation 2 may be used as a semi-empirical correlation for estimating the effect of buoyancy on triple flames with practical fuels at gravity conditions ranging from 0 to earth gravity.

### TRIPLE FLAME STABILITY

Downward-propagating triple flames at relatively strong gravity conditions have exhibited instabilities. These instabilities are generated without any artificial forcing of the flow. Instead, disturbances are initiated by minute round-off errors in the numerical simulations, and subsequently amplified by instabilities. Figure 3 shows samples of time sequence of unstable triple flames superposed on vorticity iso-contours. The figure shows that vortices originating behind the premixed branches travel downstream and consequently alter the shape of the diffusion branch.

An inviscid linear stability analysis is implemented on the steady-state triple flame solutions obtained using the formulation described above. The eigenfunction equations from the linearized disturbance equations are solved using a shooting method. The contribution of buoyancy and viscous terms are neglected in the eigenfunction analysis. The computed results for the negative imaginary part of wave number,  $-\alpha_i$ , versus frequency are presented in Figure 4. These results are based on velocity and temperature profiles at  $3\frac{1}{3}$  scalar mixing layer widths downstream of the triple flame tip with two different values of  $Fr_{L_f}$  and zero gravity. The results show that increasing the contribution of gravity in downward-propagating triple flames promotes the onset of instability, a trend that is consistent with computational observations. The most amplified frequency from stability analysis is within 15 % of the estimated value from computations. The magnitude of the frequency is lower further downstream of the premixed branches, further suggesting that instabilities originate just downstream of the premixed branches.

### ACKNOWLEDGMENTS

This work is currently supported by NASA Glenn Center for Microgravity Combustion Science.

### REFERENCES

1. Chen, J.-Y. and Echehki, T., Numerical Study of Buoyancy Effects on the Structure and Propagation of Triple Flames, to appear, *Combust. Theory Modelling*, 2001.
2. Chen, J.-Y. and Echehki, T., Proc. 5<sup>th</sup> Int. Microgravity Combustion Workshop, NASA/CP report 1999-208917 (1999).
3. Poinso, T. and Lele, S., *J. Comput. Physics*, 101: 104-129 (1992).
4. Ruetsch, G.R., Vervisch, L. and Lifan, A., *Phys. Fluids* 7(6): 1447-1454 (1995).

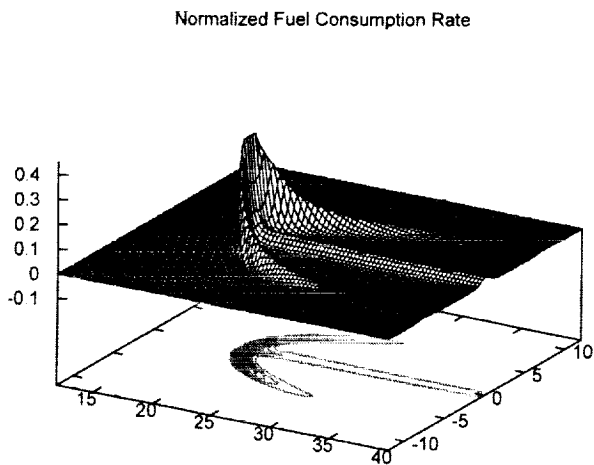


Figure 1 Computed fuel consumption rate of triple flame.

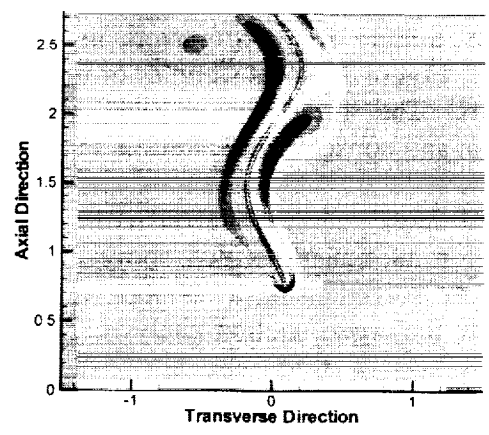
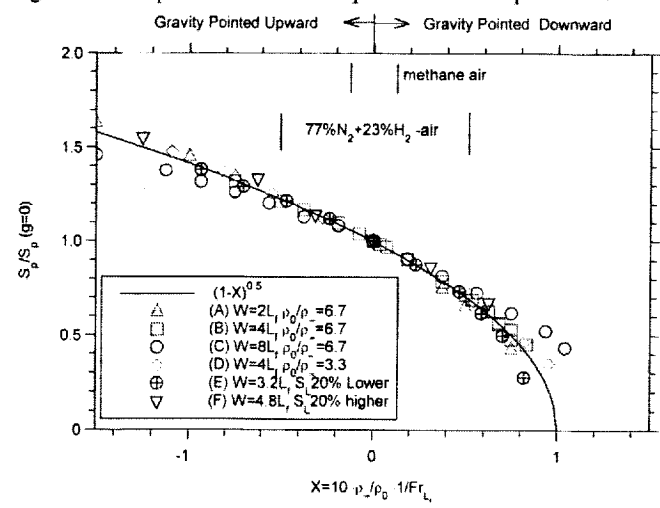
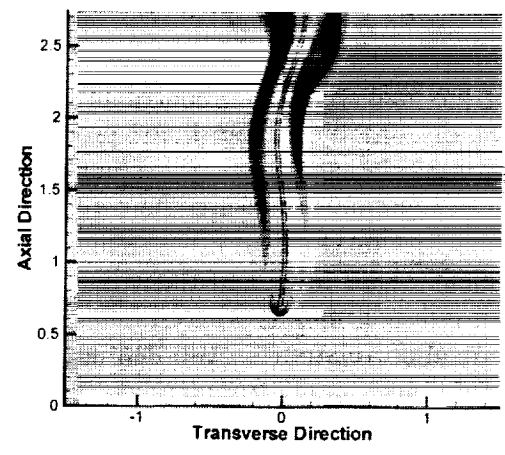


Figure 2 Correlation of flame propagation with buoyancy.

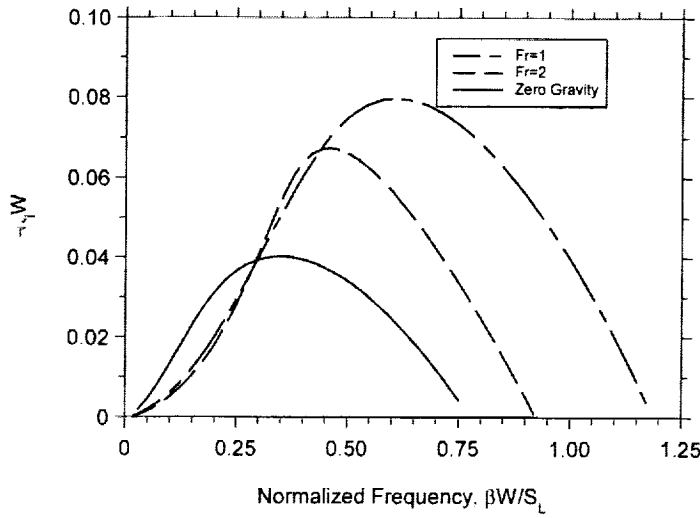


Figure 4 Linear instability analysis of triple flames.

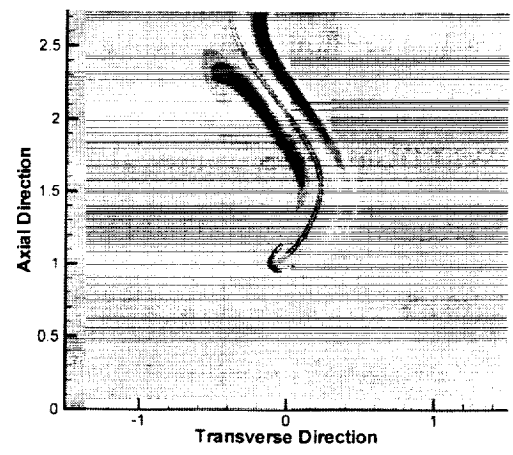


Figure 3 Unstable Triple Flames.